



STUDYING THE PROPERTIES OF WOVEN AND NON-WOVEN JUTE (*Corchorus olitorius*) FIBRE



Y. Adamu*, A. Atiku, A.D. Mahmud, A.D Ado and B. Z. Bello

Department of Chemical Engineering, Ahmadu Bello University, Zaria, Nigeria.

*Corresponding Author's Email: yusufbinadam@yahoo.com

Received: May 18, 2023 Accepted: July 31, 2023

Abstract

In this work, woven and unwoven jute fibre properties were studied. The jute plant was sourced and extracted using the wet retting method. After that, physical, chemical, mechanical properties and Weibull analysis were investigated for the single and woven jute fibres. The jute fibres were then treated using NaOH of varying % (w/v) concentrations (2, 4, 6, and 8) and then woven using a plain weave pattern. Among the treated fibres, 8% treatment gave the highest tensile strength for both single and woven jute fibre with values of 155.38 MPa and 286 MPa, respectively. The fibre water absorption test showed a gradual decrease in fibre water absorption with an increase in treatment concentration and density was found to increase with an increase in treatment concentration. The Weibull modulus for single and woven jute was found to be 16.634 and 3.4803, with characteristic strengths of 151.71 MPa and 217.02 MPa, respectively. FTIR analysis also confirmed the removal of hemicellulose, lignin, and wax as components of the treated fibres. Based on the results obtained, it is clear that jute fibre can be utilized for engineering applications.

Keywords:

Jute fibre, Chemical treatment, Mechanical properties, Weibull analysis, Peleg model and Power law model.

Introduction

Natural fibres and their syntheses have grown in popularity in industry, research, and development over the last three decades as people have become more conscious of environmental issues. An intense search for renewable and ecological engineering materials has led to these interests. (Wambua *et al.*, 2003; Summerscales *et al.*, 2010a, b; Bordoloi *et al.*, 2017a, b).

Jute fibres, along with cotton, are the most important plant fibres. The plants flourish in humid, scorching conditions. Jute is the most adaptable, environmentally friendly, abundant, high-strength, and antistatic fibre available. It consists of two species. *Corchorus capsularis* is a white jute with a silvery appearance, while *Corchorus olitorius*, is a dark jute with a golden-yellow appearance. (Mohanty *et al.*, 2005). In Nigeria, jute is known as rama (Hausa) and ewedu (Yoruba).

Jute fibres are harvested from the stem's ribbon, which is long (1.5 to 3 meters), glossy, and durable. The fibre is susceptible to bio and photo-degradation. The fibres are tough but brittle, with a low extension at break (EAB) of about 1.7 per cent. When exposed to sunlight, the fibres lose their tensile strength and are susceptible to microbes' attacks. Jute is a hygroscopic plant fibre, although it will survive a long time if kept dry. It is used as a support for walls, panelling, ceilings, and other furniture. (Bismarck *et al.*, 2005; Mohanty *et al.*, 2005; Rajasekar, 2014; Fazita *et al.*, 2017).

The retting process is used to separate jute fibre from the woody tissue of fibre crops. Retting is a technique for separating fibre tows from the central stem, allowing the fibres to be separated from the woody tissue. Fibre straw retting is caused by exposure to moisture, time, and, in some cases, the use of a mechanical decorticator. Fibre yield and fibre quality are heavily influenced by fibre separation and extraction procedures. However, there are different retting techniques exist, including mechanical, chemical, biological, and physical fibre separations (Mohanty *et al.*, 2005).

In areas with acceptable moisture and temperature ranges, dew or field retting is the most often used retting method. The dew-retting procedure can take anywhere from 3 to 6 weeks, depending on the uncontrolled weather. (Mohanty *et al.*, 2005; Placet *et al.*, 2017; Réquillé *et al.*, 2021). All retting process, which entails the fibre crop straw being submerged in heated tanks containing solutions of sulfuric acid, hydroxides of potassium or sodium, chlorinated lime etc. to dissolve the pectin in the fibre is referred to as chemical and surfactant retting. The use of surface-active chemicals in retting enables the dispersion and emulsion formation processes to easily remove undesirable non-cellulose portions sticking to the fibres. Depending on the circumstances, these actions can shorten the time it takes to ret, from 10 minutes to 48 hours. Chemical retting yields high-quality fibres but also raises the price of the finished product. (Karmakar, 1999; Bismarck *et al.*, 2005, Mohanty *et al.*, 2005).

Fibre manufacturers predominantly employ traditional cold-water retting. Anaerobic bacteria in large water tanks, ponds, rivers, etc. break down the pectin of plant straw bundles. Depending on the water type, retting water temperature, and type of bacterial inoculum, the procedure can take between 7 to 14 days. (Bismarck *et al.*, 2005; Mohanty *et al.*, 2005). Separating the bast fibres from the plant straw via mechanical or green retting is an easier and more cost-effective method. Plant straw that has been field dried but only slightly retted (2 to 3 days, but no more than 10 days) or technically dried straw is used in this technique. Mechanical techniques are used to remove the bast fibres from the woody component. Variations in fibre quality caused by the weather are eliminated. However, when compared to dew or water-retted fibres, the green fibres generated are substantially coarser and less fine. (Bismarck *et al.*, 2005; Mohanty *et al.*, 2005; Paridah *et al.*, 2011; Thomas *et al.*, 2011).

Due to the hydrophilic nature of the natural fibre, treating the fibre is necessary, to reduce the water uptake by the fibre. There are different chemical treatments carried out on fibres

which include; alkali (mercerization), acetylation, benzoylation, peroxide, and permanganate treatments (Li, *et al.*, 2007; Kabir, *et al.*, 2012; Chandrasekar, *et al.*, 2017; Abd-Halip, *et al.*, 2019). Alkali treatment of natural fibres (Equation 1) is a common approach for changing the cellulose molecular structure. The orientation of packed crystalline cellulose is altered. Alkali causes a swelling reaction in cellulosic fibres, which causes the cellulose's inherent crystalline structure to relax. Because of the swelling, alkali-sensitive hydroxyl (OH) groups contained among the molecules are broken down, react with water molecules, and subsequently move out of the fibre. (Jabbar, 2017; Chandrasekar, *et al.*, 2017; Abd-Halip, *et al.*, 2019). As a result, the hydrophilic hydroxyl groups are reduced, and the moisture resistance of the fibre is improved. Following that, rinsing with water eliminates the connected Na-ions and changes the original cellulose to cellulose-II, a new crystalline structure. A percentage of the hemicelluloses, lignin, pectin, wax, and oil covering components are also removed during this process. The aspect ratio (length or diameter) is increased as the surface roughness is increased and the fibre diameter is reduced. A higher alkali concentration than the recommended value can degrade the cellulose, affecting fibre characteristics (Yan *et al.*, 2012).
 Fibre-OH+ NaOH \longrightarrow Fibre-O⁻Na⁺ + H₂O (1)

The rate of water absorption (W), when compared to that of dry matter of the samples, can be calculated, starting from the drying mass m_0 and of the equilibrium mass m_{eq} according to Equation (3). The instantaneous humidity content $M(t)$ compared to the dry matter is calculated according to Equation (2). Equation (4) is used to calculate the ratio of the instantaneous rate of absorption, which is the equivalent without the dimension of the instantaneous water content (Ndapeu *et al.*, 2016).

$$M(t) = \frac{m(t)-m_0}{m_0} \quad (2)$$

$$w(\%) = \frac{m_{eq}-m_0}{m_0} \times 100 \quad (3)$$

$$MR = \frac{m(t)-m_0}{m_{eq}-m_0} \quad (4)$$

Where;

w (%) = Water content, m_0 = Initial dry mass (g), $m(t)$ = Mass at instant t, m_{eq} = Mass at equilibrium (g), MR = Moisture ratio.

Water absorption models

There are numerous water absorption models which include; The Pulosof, Mohsenin, Singh, Peleg, Gornicki etc. (Mbou *et al.*, 2017).

For this study, the Peleg model and Power law model are selected.

Equation (5) presents the expression of the Peleg model:

$$M(t) - M_0 = \frac{t}{k_1 + k_2 t} \quad (5)$$

Where;

k_1 is a parameter that describes the absorption kinetics, as shown in Equations (6) and (7).

$$\frac{dM(t)}{dt} = \frac{k_1}{(k_1 + k_2 t)^2} \quad (6)$$

$$\frac{dM(t)}{dt} \Big|_{t=0} = \frac{1}{k_1} \quad (7)$$

k_2 describes the equilibrium rate of absorption, when $t \rightarrow \infty$, Equation (8) is obtained.

$$M_{eq} = M_0 + \frac{1}{k_2} \quad (8)$$

This model has the advantage of being able to be expressed as an equation (9);

$$\frac{t}{M(t)-M_0} = k_1 + k_2 t \quad (9)$$

By employing Equation (9) and linear regression, the values of Peleg's parameters k_1 and k_2 can be obtained (Ndapeu *et al.*, 2016). The model can be used to accurately forecast, or at least estimate, long-term moisture gains using experimental data gathered in short-term studies (Peleg, 1988).

The power law model is given by;

$$\frac{M_t}{M_m} = k t^n \quad (10)$$

At equilibrium, M_m is the equilibrium moisture content (EMC) or water absorption at saturation point, and M_t is the moisture content at a certain time t. The numbers k and n are constants. The magnitude of n indicates whether the water diffusion through the fibre is guided by the Fickian diffusion model or not. In the log-log plot of water absorption with time, the magnitudes of k and n were evaluated as the intercept and slope, respectively, of M_t/M_m versus t (Azeez and Onukwuli, 2018).

Fibre tows can be woven in a variety of patterns when they're made. The woven fibre is made by interlacing two sets of threads: longitudinal (or warp) threads and latitudinal (or weft) threads, at right angles in the same plane. The warp threads are sewn together into a sheet, parallel to each other. This warp sheet must be 'shed', that is, separated and parted to form an upper (or front) sheet and a lower (or rear) sheet, to permit interlacement with weft threads. Between these two sheets lies a path of weft thread. The two sheets are 'unshed' and rejoined as a single sheet, allowing the inserted weft to interlace with the warp sheet's threads (Hann and Thomas, 2005; Coleman and Hann, 2008; Kubley *et al.*, 2019).

Fibres cannot be studied, without studying the probabilities of failure. The Weibull Probability Analysis is used to investigate the variance in tensile strength of brittle materials, which is frequently represented by the Weibull Probability Distribution (WPD). It's been used on synthetic and natural textiles material. The WPD's goal is to find the shape and scale parameters that best fit the experimental data distribution. The strength variability is described by the form parameter, also known as the Weibull modulus; a higher value of the Weibull modulus suggests less strength variability (Ibrahim *et al.*, 2018).

To plot the Weibull plot, the tensile test result is used. The Weibull distribution with two parameters is known as the common two-parameter distribution;

$$F(\sigma) = 1 - \exp\left(-\frac{L}{L_0} \left(\frac{\sigma}{\sigma_0}\right)^m\right) \quad (11)$$

$$\ln\left(\ln\left(\frac{1}{1-F(\sigma)}\right)\right) - \ln\left(\frac{L}{L_0}\right) = m(\ln\sigma - \ln\sigma_0) \quad (12)$$

Where; F (σ) is the fibre's failure probability. L is the reference length and L_0 is the initial fibre length, σ and σ_0 are, respectively, applied stress and characteristic strength (scale parameter). While m is the Weibull modulus. For a constant gage length, Equation (12) becomes;

$$\ln\left(\ln\left(\frac{1}{1-F(\sigma)}\right)\right) = m(\ln\sigma - \ln\sigma_0) \quad (13)$$

The value of the x-axis ($x = \ln \sigma$) is a transformation logarithmic of the stress and the y-axis is defined by equation (14):

$$y = \ln \left(\ln \left(\frac{1}{1-F(\sigma)} \right) \right) \quad (14)$$

The Weibull modulus, m and characteristic strength, σ_0 were derived from the gradient and the exponential of the intercept over gradient of the plot of $\ln \sigma$ versus $\ln \left(\ln \left(\frac{1}{1-F(\sigma)} \right) \right)$

Bernard's approximation (15) is applied to determine the median ranks.

$$F(\sigma) = \frac{i-0.3}{N+0.4} \quad (15)$$

where i is the rank of each data point and N is the total number of samples.

Materials and Methods

Materials

The jute plant was sourced from National Research Institute for Chemical Technology (NARICT), Basawa, in Zaria, Nigeria. Resin silicate (Na_2SiO_3) (Alderich reagent grade), Potassium Alum ($\text{KAl}(\text{SO}_4)_2 \cdot 12\text{H}_2\text{O}$) (Alderich reagent grade). Polysaccharide (starch) (Alderich reagent grade) and Sodium hydroxide (NaOH) pellets (98 %) were bought from Haddis International, Samaru Zaria.

Plates I – IX shows pictorial illustrations of the extraction process and some equipment used.

Methods

Extraction of jute fibre

The cold-water retting process described by Mohanty *et al.*, 2005 was adopted. Dried jute bark was scraped from a jute stick and the jute bark was soaked in water for 3 weeks and resulting fibres were obtained by combing. The fibres were then sun-dried for 24 hours.

Chemical treatment of jute fibres

Jute fibre samples were divided into 4 and weighed 200 g each using the Metlar MT-501 electronic balance and then treated with 2 %, 4 %, 6 %, and 8 % (w/v) NaOH solution for 30 minutes each at room temperature and then washed thoroughly with fresh water and allowed to dry at room temperature for 24 hours (Naveen *et al.*, 2015).

The weaving of jute fibres

The NaOH-treated fibres have further added some additives like resin silicate (Na_2SiO_3) which acts as a binder in the formation of the jute yarn, fibres were also added potassium alum ($\text{KAl}(\text{SO}_4)_2 \cdot 12\text{H}_2\text{O}$) and polysaccharide to enable swift twisting and to add strength to them to avoid breakage during weaving. The twisted fibres were then woven into a plain weave pattern using the vertical hand loom in the Department of Textile and Industrial Design, Ahmadu Bello University, Zaria.



Plate I: Retting.



Plate II: Alkali treatment.



Plate III: Retted jute bark.



Plate IV: Combing



Plate V: Drying of treated fibres.



Plate VI: Sorting and drying.



Plate VII: Weighed portion of the dried fibre.



Plate XIII: Fibre placed in jaws.



Plate IX: Fibre fracture after load application.

Tests and analysis

Fourier transform infrared spectrometry (FTIR) analysis

To validate the elimination of non-cellulosic materials (e.g., hemicellulose and lignin) from alkali-treated woven jute fibre, FTIR spectroscopic analysis was performed on the treated fibres and untreated fibre. The functional groups of both treated and untreated jute fibre were analyzed using a Shimadzu machine (model: FTIR-84005) FT-IR spectrometer after the treated samples were dried. To eliminate the moisture, the samples were dried in an oven at 60°C. On a KBr plate, around 0.5 mg of the specimens were deposited and inserted into the infrared barrel. These samples' infrared spectra were measured in the transmission of wavelengths ranging from 4000 to 500 cm^{-1} .

Tensile test

Single strands of jute fibres of thickness 0.05 mm and 100 mm gauge length each of untreated and chemically treated samples was tested using the universal tester Model WDS-3kN according to ASTM D 3822, using sample dimension 100 mm x 0.05 mm. The average values were recorded and tabulated. The samples of woven fabric were also tested. A tensile test was carried out as per ASTM D 5035-06. Samples of woven jute fabric were cut to dimensions of (150 mm x 25 mm x 3 mm), the gauge length was set to 75 mm and the loading speed was set to 200 mm/min. The test was carried out with a universal tester and the average values were recorded and tabulated.

Density test

A density test was carried out on the woven jute fabric according to ASTM D 792-08. The density was calculated using the formula $\text{density} = \frac{\text{mass (g)}}{\text{volume (cm}^3\text{)}}$. The mass of each sample was recorded before water immersion and then removed after some time and the volume of the water displaced is recorded.

Water absorption test and models

To study the behaviour of water absorption of the woven jute fibre, a water absorption test was carried out according to ASTM D 570-98 for the 0 %, 2 %, 4 %, 6 % and 8 % (w/v) NaOH-treated samples. The repeated immersion method is used. Each of the samples was dried at room temperature until they have a constant mass (m_0) and the weight was recorded. They were then each immersed in water and weighed (m_t), the water immersion was repeated at time intervals of 2, 4 and 24 hours. The percentage weight gained was calculated using Equation 3. For the water absorption models,

Peleg model

After calculating the % water absorption of woven fibres at different time intervals, the % of water absorbed at time t (m_t) and initial moisture absorption (m_0) are used in Equation 5, and a graph of $t(m_t - m_0)$ vs time was plotted to obtain R^2 , k_1 and k_2 .

Power law model

The weight gained at each time interval (m_t) and weight of the sample at saturation (m_n) is used in Equation 10, while the graph of $\ln(m_t/m_n)$ is plotted against $\ln(\text{time})$ to obtain the values of n and k .

Weibull analysis of tensile strength

Weibull distribution analysis was used to find the shape and scale parameters that best fit the distribution of the experimental data. Equation 11 is used to plot the Weibull plot using the tensile test data. For a constant gage length, this was reduced to Equation 12. The Weibull modulus, m and characteristic strength, σ_0 were derived from the gradient and the exponential of the intercept over gradient of the plot of $\ln \sigma$ versus $\ln\left(\frac{1}{1-F(\sigma)}\right)$. The failure probability of the fibre $F(\sigma)$ is also determined using Equation 15 and the values obtained are tabulated.

Results and Discussion

Fourier transform infrared spectrometry of treated and untreated jute fibre

Figure 1, shows the region of the broad absorption band for untreated and treated fibres at 3300 cm^{-1} to 3500 cm^{-1} is characterized by O-H stretching and H-bonded bond structure, which primarily contains major functional groups of alcohols, phenols, and waters. After alkaline treatment, the O-H stretching and H-bonded broad absorption band in the region are reduced. The reduction in intermolecular and intramolecular hydrogen bonding between the hydroxyl groups of cellulose and hemicellulose of jute fibre due to alkali treatment implies a reduction in intermolecular and intramolecular hydrogen bonding between the hydroxyl groups of cellulose and hemicellulose of jute fibre. From Table 1, the untreated shows a peak wavenumber of 3287.5 cm^{-1} while the 2% treated is 3280.1 cm^{-1} and 3272.6 cm^{-1} for the 8% treated. Also from the table, the peak wavenumbers of 2918.5 cm^{-1} and 2109.7 cm^{-1} indicate methoxy, C-H stretch ($\text{CH}_3\text{-O}$). The wavenumber 1722.0 cm^{-1} indicates carboxylic acid. Furthermore, the peak wavenumbers of 1595.3 cm^{-1} and 1509.6 cm^{-1} indicate C=C. Aromatic ring stretch (lignin) and the absence of 1509.6 cm^{-1} stretch for both the 2% and 8% treated indicates the removal of some lignin. The wavenumber 1367.9 cm^{-1} represents CH_2 stretching (cellulose, hemicellulose, and lignin), which is eliminated in the 2% and 8% treated fibres. The peak of 1241.2 cm^{-1} indicates aromatic ethers and aryl-O stretch, and this is absent in the 2% and 8% treated jute fibres, indicating its removal. This is in agreement with Singh (2019), who reported that after surface treatment of jute fibres with NaOH, FTIR results showed that there was no triple bond functional group, which confirmed the removal of cellulose, hemicellulose, and lignin.

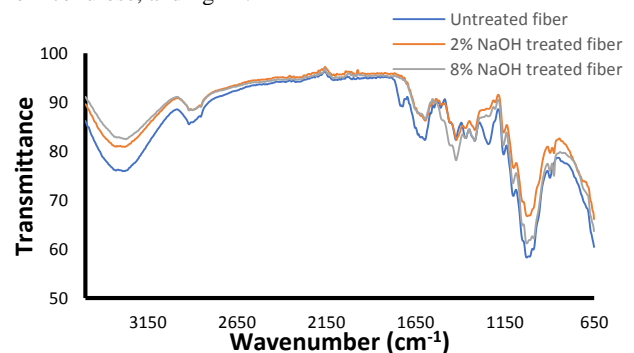


Figure 1: FTIR results for selected fibre concentrations treatment.

Table 1: Wavenumbers and their characteristic functional groups.

S/N	Characteristics	Wavenumber (cm ⁻¹)		
		Untreated	2 % treated	8 % treated
1	Hydroxy group, H-bonded OH stretch	3287.5	3280.1	3272.6
2	Methoxy, C-H stretch (CH ₃ -O-) Ether	2918.5 & 2109.7	2918.5	2918.5
3	Carboxylic acid	1722.0	-	-
4	C=C-Aromatic ring stretch	1595.3	1595.3	1595.3
5	C=C-Aromatic ring stretch alkene (lignin)	1509.6	-	-
6	C-H deformation	1423.8	1420.1	1423.8
7	CH ₂ stretching (cellulose, hemicellulose and lignin)	1367.9	-	-
8	Carbonyl compounds	1319.5	1319.5	1319.5
9	Aromatic ethers, aryl -O stretch	1241.2	-	-
10	Secondary amine, CN stretch	1155.5	1155.5	1155.5

Tensile strength test

Table 2: Tensile test result for a single strand of jute fibres.

S/N	NaOH concentration (%)	Tensile strength (MPa)	Breaking force (N)
1	0	134.12	670.6
2	2	146.57	732.85
3	4	148.75	743.75
4	6	155.23	776.15
5	8	155.38	776.9

The result of the tensile test for a single strand of single fibres as shown in Table 2 shows a gradual increase in the tensile strength of fibres, which shows the effectiveness of the NaOH treatment of fibres. The best treatment concentration which shows the highest tensile strength is 8

(155.38 MPa). This is in agreement with Roy et al. (2012), who also reported that mild alkali treatment of jute fibre improved its tensile characteristics, and alkali treatment caused non-cellulosic components to leach away, which was the main reason for the fibre's improved tensile capabilities.

Table 3: Average tensile test analysis of woven jute fabric.

S/N	NaOH %	Tensile Strength (MPa)	Elastic Modulus (MPa)	Elongation %	Yield Strength (MPa)	Max load (KN)
1	0	6.02	22.59	27.67	4.04	0.68
2	2	7.62	16.99	56.17	7.24	0.80
3	4	8.50	19.79	49.41	1.33	0.89
4	6	10.35	20.69	37.34	9.71	1.08
5	8	14.88	53.89	21.60	5.63	1.43

To compare the tensile strength of both the single and woven jute we have to scale down the woven jute area to about 5 mm² which is the area of the single jute strand. The average area of all the woven jute is (75 mm x 35 mm) which is 2625 mm². By scaling down the area in the ratio 1:525, we divide the woven jute area by 525 and we get an area of 5 mm² which is equivalent to that of the single strand. The new tensile strength of the woven jute is now calculated using the breaking strength from Table 3 and the 5 mm² area using the formula.

$$\text{tensile strength} = \frac{\text{Breaking force(N)}}{\text{area(mm}^2\text{)}} \quad (16)$$

The new tensile strength values are recorded in Table 4.

Table 4: Calculated tensile strength values for woven jute.

S/N	NaOH %	Tensile strength (MPa)
1	0	136
2	2	160
3	4	178
4	6	216
5	8	286

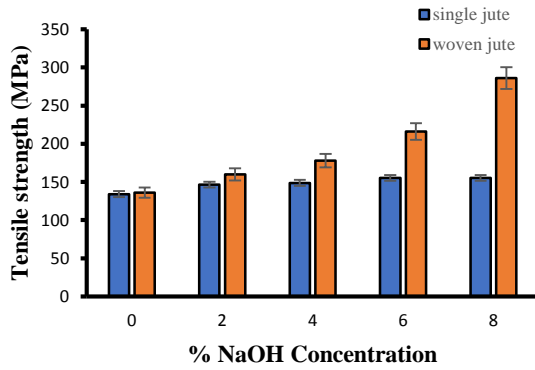


Figure 2: Comparison of tensile strength for single strand and woven jute fibre.

From Figure 2, it can be seen that with an increase in alkali treatment concentration, there is a gradual increase in all the tensile strengths of both the woven and unwoven fibres. At 0 % alkali concentration, there is a 1.49 % increase in the tensile strength of the woven jute over the single strand. At 2% alkali concentration, the tensile strength of the woven jute is higher than that of the single strand by 9.16%. At 4% alkali concentration, the woven jute tensile strength is higher than that of the single strand by 19.66%. At 6% alkali concentration, the woven jute tensile strength is higher than that of the single strand by 39.14%. Finally, at 8% alkali concentration, the woven jute tensile strength is 84.06% greater than the single strand. The large increment in the tensile strength of the woven jute fibres over the unwoven is due to some factors like alkali treatment, the weave pattern, the chemical adhesives added during weaving pretreatment, and the large bundle of fibres in single jute twine.

Density test for treated and treated jute fibre

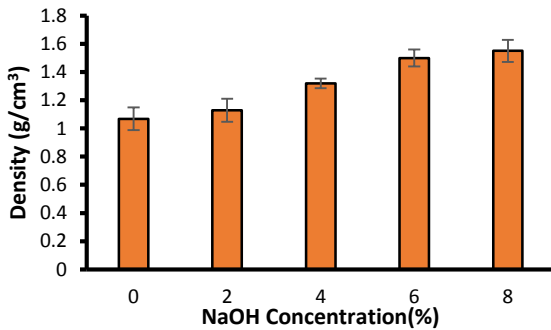


Figure 3: Variation of density with NaOH concentration treatment.

Figure 3 depicts the density of woven jute fibres at various alkali treatment concentrations. The results demonstrate that after the alkali treatment process, the density of jute fibres increased slightly. This positive change or increment in fibre density normally signifies cell wall densification. The density of the woven treated fibres compared to the untreated woven jute increased by 14.54 %, 36.72 %, 45.21 %, and 56.33 % for the 2 %, 4 %, 6 %, and 8 % alkali-treated fibres. This is in agreement with Hashim et al. (2017), who stated that the density of kenaf fibre under various alkali treatment settings exhibits a progressive increment pattern at tiny amounts with the increment of all treatment parameter values.

Water absorption analysis for treated and treated jute fibre

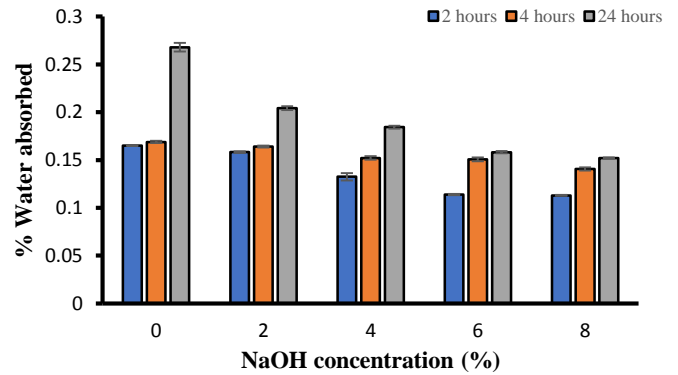


Figure 4: Effect of NaOH treatment concentration on fibre water absorption.

From Figure 4 above, it can be seen that after two hours, the untreated woven jute has a percentage water absorption of 0.1650% while the alkali-treated woven samples (2, 4, 6, and 8 %) have a percentage water absorption of 0.1583 %, 0.1326 %, 0.1138 %, and 0.1130 %. After 4 hours, the untreated woven sample has a percentage water absorbed of 0.1690 % while the treated (2, 4, 6, and 8 %) woven samples have a percentage water absorbed of 0.1641 %, 0.1522 %, 0.1507 %, and 0.1408 %. Finally, after 24 hours, the percentage of water absorbed by the untreated woven sample is 0.2680 %, while that of the alkali-treated samples of 2, 4, 6, and 8 % has a percentage of water absorbed of 0.2043 %, 0.1844 %, 0.1582 %, and 0.1521 %. By analyzing all the data above, it can be seen that alkali treatment reduced the hydrophilic nature of jute fibre. This is in agreement with Roy et al. (2012), who reported that the moisture content of jute fibre decreased as the concentration of alkali solution and duration of treatment increased.

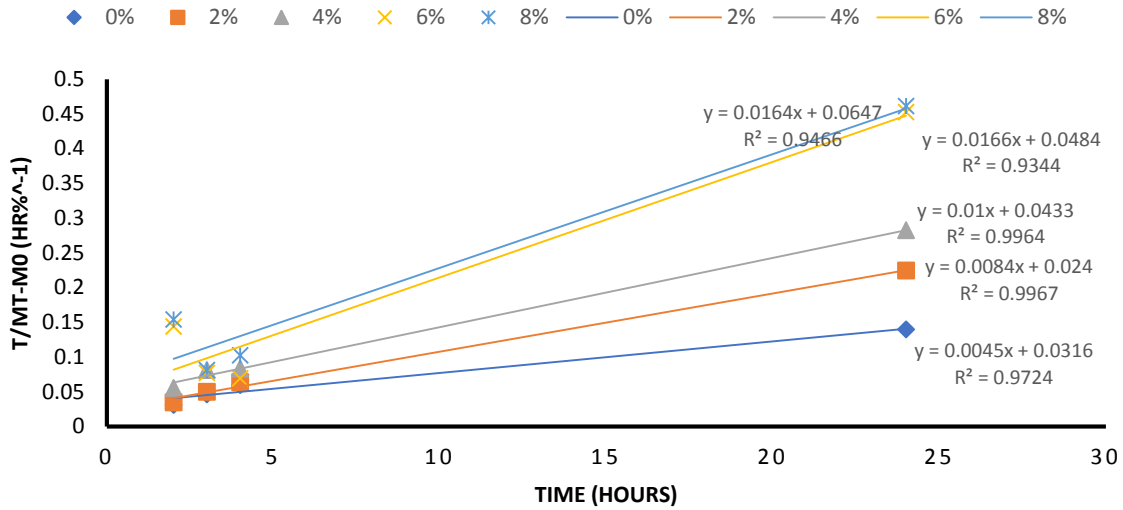


Figure 5: Peleg model graph for water absorption.

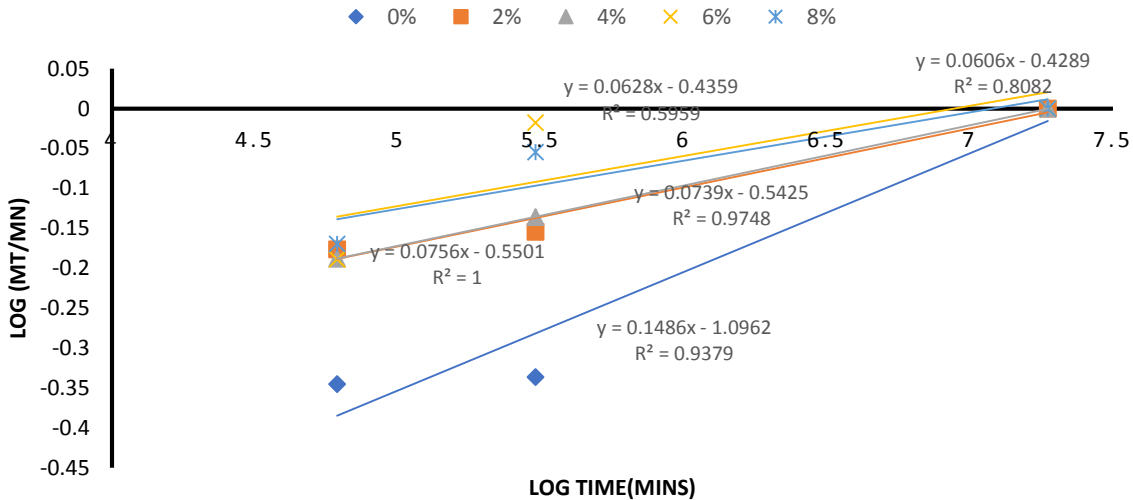


Figure 6: Power law model plot.

Table 5: Parameter values for the Peleg model

S/N	NaOH concentration %	R ²	k ₁ (hr.% ⁻¹)	k ₂ (% ⁻¹)
1	0	0.9724	0.0316	0.0045
2	2	0.9967	0.0240	0.0084
3	4	0.9964	0.0433	0.0100
4	6	0.9344	0.0484	0.0166
5	8	0.9466	0.0647	0.0164

The results of water absorption of the woven jute of different NaOH % (w/v) treatments were used to plot the Peleg graph as shown in Figure 5. From the graph, the parameter values of R², k₁ and k₂ were calculated and tabulated in Table 5. Figure 5 shows that Peleg's model accurately described the water sorption kinetics of untreated and treated fibres due to the high value of R². The Peleg constants k₁ (water absorption rate) and k₂ (capacity constant) can be used to successfully predict the water absorption behaviour of the fibres at any time t using Equation 5.

The untreated woven jute has the lowest k₁ (0.0316 hr.%⁻¹) and thus has the highest initial water absorption rate while 8 % treated woven jute has the highest k₁ (0.0647 hr.%⁻¹) which indicates the lowest initial water absorption rate. The k₂ is related to maximum water absorption capacity that is, the lower the k₂, the higher the absorption capacity. Also, from Table 5 the untreated woven jute has the lowest k₂ (0.0045 %⁻¹) which means it has the highest water absorption capacity while the 6 % treated has the highest k₂ (0.0166%⁻¹) which means it has the lowest water absorption capacity. This is in agreement with Azeez and Onukwuli, (2018) who

reported that NaOH modification reduced the water absorption capacity of fibres.

Table 6: Parameter values for the power-law model

S/N	% NaOH concentration	R ²	n (mins ⁻¹)	K
1	0	0.9379	0.1486	0.3341
2	2	0.9748	0.0739	0.5813
3	4	1.0000	0.0756	0.5769
4	6	0.5959	0.0628	0.6467
5	8	0.8082	0.0606	0.6512

The results of water absorption of the woven jute of different NaOH % (w/v) treatments were used to plot the power-law-model graph as shown in Figure 6. From the graph, the parameter values of R², n (sorption index) and k (sorption rate constant) were calculated and tabulated in Table 6. These parameters n and k are used to successfully predict the water absorption of fibres at any time t using Equation 10. Also, from Table 6 it can be seen that the water absorption index decreases with an increase in NaOH % concentration. According to this model, the jute fibre with the least water absorption index n is the 8 % treated woven jute. It can be concluded that untreated and treated jute fibres exhibit less Fickian behaviour since n < 0.5 (water penetration rate is much more below fibre relaxation rate). This is in agreement with the report of Gierszewska-Drużyńska and Ostrowska-Czubenko, (2012).

Therefore, NaOH treatment reduces the sorption rate constant (k) with an increase in sorption index (n). This could be due to fibre source and processing, fibre shrinkage, porosity or void development, and hemicellulose and lignin content reduction, all of which cause jute fibres to become more hydrophobic, as stated by Azeez and Onukwuli (2018).

Weibull analysis of tensile strength

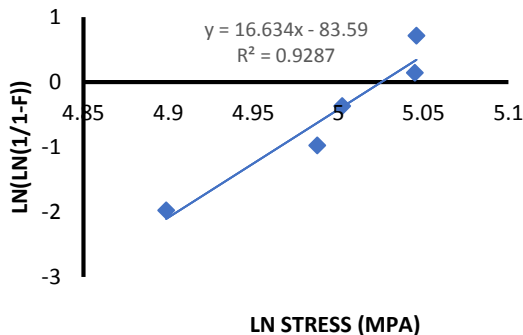


Figure 7: Weibull probabilities graph for Single Strand Fibre.

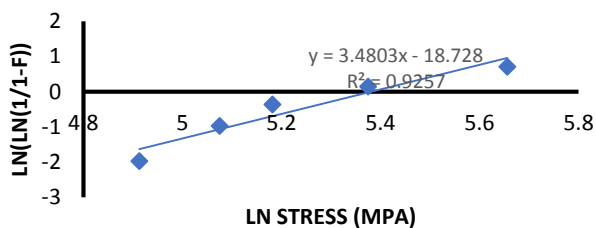


Figure 8: Weibull probabilities graph for woven jute fibre.

The result of tensile strength was used to plot the Weibull graph. A graph of ln(ln(1/(1-F))) was plotted against ln stress as shown in Figures 7 and 8. From the graphs, it can be seen that the R² values for woven and unwoven are 0.9257 and 0.9287, which are the reliability factors and are very good due to their closeness to 1. The Weibull modulus ‘m’ was also found to be 3.4803 and 16.634. The characteristic strength, which is the exponential of the intercept from the graph (5.38 and 5.022 MPa), was also calculated and found to be 217.022 and 151.71 MPa for woven and unwoven jute fibre, respectively. The results from the Weibull analysis are in agreement with the work of Ibrahim et al. (2018). Table 7 gives the summary of the parameter values from the Weibull graph.

Table 7: Summary of the parameter values for single strand and woven jute Weibull graph

Fibre Nature	R ²	M	Intercept (MPa)
Unwoven	0.9287	16.634	5.022
Woven	0.9257	3.4803	5.38

To summarize, the higher the Weibull modulus, the more consistent the material (i.e., uniform defects are evenly distributed across the material) and the smaller the probability curve of the strength distribution (as seen in Figure 7). Weibull modulus values for most natural fibres should be in the range of 1 to 6 (Ibrahim *et al.*, 2018).

Conclusion

The properties of the woven jute fibre were investigated in this work by varying the sodium hydroxide treatment concentrations. Based on the results obtained, the following conclusions were drawn:

- The fibres sourced from the jute plant were successfully extracted from jute bark using cold water retting process.
- The jute fibres were treated using sodium hydroxide of varying concentrations of 2, 4, 6 & 8 % (w/v) and woven using a plain weave pattern. Woven and unwoven jute fibres treated with 8 % w/v NaOH had the highest tensile strength of 286 MPa and 155.38 MPa respectively.
- The density of woven jute increased slightly with an increase in alkali treatment concentration. woven jute treated with 8 % w/v NaOH has the highest density (1.722 g/cm³) compared to untreated woven jute (1.102 g/cm³). Also, at the same concentration after 24 hours, the water absorption values were 0.1521 % and 0.2680 % for treated and untreated fibre respectively.
- The Peleg model showed that the untreated woven jute has the highest initial water absorption rate and absorption capacity. While 6 % and 8 % treated woven jute have the lowest initial water absorption rate and absorption capacity respectively.
- The power law model showed that the 0 % and 8 % treated had the highest and lowest water absorption index (n) of 0.1486 mins⁻¹ and 0.0606 mins⁻¹ respectively. While the FTIR analysis conducted on both the treated and untreated jute fibres showed the removal of some cellulosic components.

- Weibull analysis for the woven and unwoven jute fibre showed a Weibull modulus and characteristic strength of 3.4803, 217.022 MPa and 16.634, 151.71 MPa respectively. Therefore, it can be concluded that the tensile strength and water absorption for the woven and unwoven jute fibres all improved significantly with the alkali treatment.

References

- ASTM D3822 – Standard Test Method for Tensile Properties of Single Textile Fibre, 2007
- ASTM D 5035-06. Standard Test Method for Breaking Force and Elongation of Textile Fabrics (Strip method) (Reapproved 2008).
- ASTM D 792-08. Standard Test Methods for Density and Specific Gravity (Relative Density) of Plastics by Displacement.
- ASTM D 570-98. Standard Test Methods for Water Absorption of Plastics.
- Ahmed, A. S., Islam, S., Hassan, A., Haafiz, M. K. M., Nurul Islam, K., & Arjmandi, R. (2013). Impact of Succinic Anhydride on the Properties of Jute Fibre / Polypropylene Biocomposites. *Fibres and Polymers*, 15(March 2014), 307–314. <https://doi.org/10.1007/s12221-014-0307-8>
- Azeez, T. O., & Onukwuli, D. O. (2018). Properties of White Roselle (*Hibiscus sabdariffa*) Fibres. *Journal of Scientific & Industrial Research*, 77(September), 525–532.
- Abd Halip, J., Hua, L. S., Ashaari, Z., Tahir, P. M., Chen, L. W., & Uyup, M. K. A. (2019). Effect of treatment on water absorption behaviour of natural fibre–reinforced polymer composites. In *Mechanical and physical testing of biocomposites, fibre-reinforced composites and hybrid composites* (pp. 141-156). Woodhead Publishing.
- Bismarck, A., Mishra, S., & Lampke, T. (2005). Plant fibres as reinforcement for green composites. In *Natural fibres, biopolymers, and biocomposites* (pp. 52-128). CRC Press.
- Bordoloi, S., Garg, A., and Sekharan, S. (2017a). “A review of physio-biochemical properties of natural fibres and their application in soil reinforcement,” *Advances in Civil Engineering Materials* 6(1), 323-359. DOI: 10.1520/ACEM20160076
- Bordoloi, S., Hussain, R., Sen, S., Garg, A., and Sreedeeep, S. (2017b). “Chemically altered natural fibre impregnated soil for improving subgrade strength of pavements,” *Advances in Civil Engineering Materials* 7(2). DOI: 10.1520/ACEM20170042
- Coleman, H., & Hann, M. A. (2008). *Patterns of Culture: The Textiles of Bali and Nusa Tenggara*. University of Leeds.
- Chandrasekar, M., Ishak, M. R., Sapuan, S. M., Leman, Z., & Jawaid, M. (2017). A review on the characterisation of natural fibres and their composites after alkali treatment and water absorption. *Plastics, Rubber and Composites*, 46(3), 119-136.
- Fazita, M. N., Khalil, H. A., Wai, T. M., Rosamah, E., & Aprilia, N. S. (2017). Hybrid bast fibre reinforced thermoset composites. In *Hybrid Polymer Composite Materials* (pp. 203-234). Woodhead Publishing.
- Gierszewska-Drużyńska M & Ostrowska-Czubenko J. (2012) Mechanism of water diffusion into non-crosslinked and ionically crosslinked chitosan membranes, *Prog Chem and Appl Chitin Derivatives*, XVII 59 – 66.
- Hann, M. A., & Thomas, B. G. (2005). *Patterns of Culture, Decorative Weaving Techniques*. The University of Leeds.
- Ibrahim, I., Sarip, S., Bani, N. A., Ibrahim, M. H., & Hassan, M. Z. (2018). *The Weibull probabilities analysis on the single kenaf fibre*. 020009(May 2018), 8. <https://doi.org/https://doi.org/10.1063/1.5034540>
- Jabbar, A. (2017). *Sustainable Jute-Based Composite Materials: Mechanical and Thermomechanical Behaviour*. SpringerBriefs.
- Kabir, M. M., Wang, H., Lau, K. T., & Cardona, F. (2012). Chemical treatments on plant-based natural fibre reinforced polymer composites: An overview. *Composites Part B: Engineering*, 43(7), 2883-2892.
- Karmakar, S. R. (1999). *Chemical technology in the pre-treatment processes of textiles*. Elsevier.
- Kubley, A., Chauhan, D., Kanakaraj, S.N., Shanov, V., Xu, C., Chen, R., Ng, V., Bell, G., Verma, P., Hou, X. and Chitranshi, M., (2019). Smart textiles and wearable technology innovation with carbon nanotube technology. In *Nanotube Superfibre Materials* (pp. 263-311). William Andrew Publishing.
- Li, X., Tabil, L. G., & Panigrahi, S. (2007). Chemical treatments of natural fibre for use in natural fibre-reinforced composites: a review. *Journal of Polymers and the Environment*, 15(1), 25-33.
- Mbou, E. T., Njeugna, E., Kemajou, A., Sikame, N. R. T., & Ndapeu, D. (2017). *Modelling of the Water Absorption Kinetics and Determination of the Water Diffusion Coefficient in the Pith of *Raffia vinifera* of Bandjoun , Cameroon*. 2017.
- Mohanty, A. K., Misra, M., & Drzal T. L. (2005). *NATURAL FIBRES , BIOPOLYMERS , AND BIOCOSITES*.
- Naveen, E., Venkatachalam, N., & Maheswaran, N. (2015). Alkalicchemical Treatment on the Surface of Natural Fibre. *International Journal of Innovative Research in Science, Engineering and Technology*, 4(4), 172–178.
- Ndapeu, D., Njeugna, E., Sikame, N. R., Bistac, S. B., Drean, J. Y., & Fogue, M. (2016). Experimental Study of the Water Absorption Kinetics of the Coconut Shells (*Nucifera*) of Cameroun. *Material Sciences and Applications*, 7(March), 159–170.
- Paridah, M. T., Basher, A. B., SaifulAzry, S., & Ahmed, Z. (2011). Retting process of some bast plant fibres and its effect on fibre quality: A review. *BioResources*, 6(4), 5260-5281.
- Peleg, M. (1988). An Empirical Model for the Description Moisture Sorption Curves. *JOURNAL OF FOOD SCIENCE*, 53(4), 1216–1217.

- Placet, V., Day, A., & Beaugrand, J. (2017). The influence of unintended field retting on the physicochemical and mechanical properties of industrial hemp bast fibres. *Journal of Materials Science*, 52(10), 5759-5777.
- Rajasekar, K. (2014). Experimental Testing Of Natural Composite Material (Jute Fibre). *IOSR Journal of Mechanical and Civil Engineering*, 11(2), 1–9.
- Réquilé, S., Mazian, B., Grégoire, M., Musio, S., Gautreau, M., Nuez, L., Day, A., Thiébeau, P., Philippe, F., Chabbert, B. and Chamussy, A., (2021). Exploring the dew retting feasibility of hemp in very contrasting European environments: Influence on the tensile mechanical properties of fibres and composites. *Industrial Crops and Products*, 164, p.113337.
- Roy, A., Chakraborty, S., Kundu, S. P., Basak, R. K., Majumder, S. B., & Adhikari, B. (2012). Improvement in mechanical properties of jute fibres through mild alkali treatment as demonstrated by utilisation of the Weibull distribution model. *Bioresource Technology*, 107, 222–228. <https://doi.org/10.1016/j.biortech.2011.11.073>
- Singh, S. P. (2019). FTIR Spectroscopy & Mechanical Behaviour Study on Jute Fibre Polymer Composite. *Journal of Advanced Engineering Research*, 6(1), 34–38.
- Summerscales, J., Dissanayake, N. P. J., Virk, A. S., and Hall, W. (2010a). “A review of bast fibres and their composites. Part 1 – Fibres as reinforcements,” *Composites Part A: Applied Science and Manufacturing* 41(10), 1329-1335. DOI: 10.1016/j.compositesa.2010.06.001
- Summerscales, J., Dissanayake, N., Virk, A., and Hall, W. (2010b). “A review of bast fibres and their composites. Part 2 – Composites,” *Composites Part A: Applied Science and Manufacturing* 41(10), 1336-1344. DOI: 10.1016/j.compositesa.2010.05.020
- Thomas, S., Paul, S. A., Pothan, L. A., & Deepa, B. (2011). Natural fibres: structure, properties and applications. In *Cellulose fibres: bio-and nano-polymer composites* (pp. 3-42). Springer, Berlin, Heidelberg.
- Wambua, P., Ivens, J., and Verpoest, I. (2003). “Natural fibres: Can they replace glass in fibre reinforced plastics?” *Composites Science and Technology* 63(9), 1259-1264. DOI: 10.1016/S0266-3538(03)00096-4. www.marketizer.com/usesandapplicationsofliquidandsolidsoxidiumsulfate
- Yan, L., Chouw, N., & Yuan, X. (2012). *Improving the mechanical properties of natural fibre fabric reinforced epoxy composites by alkali treatment*. <https://doi.org/10.1177/0731684412439494>